Geophysica (2019), 54(1), 93–105

Station Calibration of the SWEPOS GNSS Network

Martin Lidberg[1], Per Jarlemark[2], Jan Johansson[2,3], Kent Ohlsson[1], Lotti Jivall[1] and Tong Ning[1]

[1] Lantmäteriet. SE-801 82 Gävle, Sweden
[2] RISE Research Institute of Sweden. Box 857, SE-501 15 Borås, Sweden
[3] Chalmers University of Technology. Onsala Space Observatory, SE-439 92, Onsala

(Submitted: November 1, 2018; Accepted: May 15, 2019)

Abstract

The performance of GNSS based positioning services is improving to the benefit of the users, and the uncertainties from densified RTK networks for construction work is approaching the sub-centimeter level also in the vertical. The error sources related to the continuously operating reference stations (CORS) may therefore soon be limiting factors for further improvement of performance. Station dependent effects are thus important in high accuracy GNSS positioning. Electrical coupling between the antenna and its near-field environment changes the characteristics of the antenna from what has been determined in e.g. absolute robot or chamber calibrations.

Since the first initial tests back in 2008, Lantmäteriet together with Chalmers University of Technology and Research Institute of Sweden (RISE), has carried out in-situ station calibration of its network of permanent reference stations, SWEPOS. The station calibration intends to determine the electrical center of the GNSS antenna, as well as the PCV (phase center variations) when the antenna is installed at a SWEPOS station. One purpose of the calibration is to examine the site-dependent effects on the height determination in SWEREF 99 (the national reference frame). Another purpose is to establish PCV as a complement to absolute calibrations of the antenna-radome pair.

In this paper we present both the methodology for observation procedure in the field and the method for the analysis, together with results of the station-dependent effects on heights as well as PCV from the analysis. Some strength and weakness of our method for GNSS station calibration are discussed at the end.

Keywords: GNSS, Antenna calibration, site dependent effects, local tie

1 Introduction

Site-dependent effects are important in high-accuracy GNSS positioning. Electrical coupling between the antenna and its near-field environment could change the characteristics of the antenna from what has been determined for the isolated antenna (*Wübbena et al*., 2010, *Wübbena and Schmitz*, 2011). The average position of apparent signal reception, the phase center offset (PCO) and the directional dependent phase center variations (PCV) (*Rothacher and Mader,* 2003) derived for the antenna in e.g. absolute calibration may not be valid when it is mounted for a permanent use. The actual differences in range caused by the near field effects may only be some millimeters, but the coordinate bias may reach centimeters. An increase by a factor of three is generally due to the use of the ionospheric free linear combination (L3). Limitations in the PCV model may cause additional biases that are amplified when estimating e.g. tropospheric zen-

ith delays (*Wübbena and Schmitz*, 2011). In-situ calibration of GNSS stations is therefore required for the most demanding applications (*Wübbena et al*., 2010).

The early study by *Elósegui et al*. (1995) discussed multipath and near field scattering and investigated the effect by analyzing the baseline between an antenna installed on a concrete pillar and a nearby antenna on a wooden survey tripod. The computed baseline (~2.2 m) was sensitive to the elevation cut off angle, where the vertical coordinate changed by 9.7 ± 0.8 mm when the elevation cut off angle was increased from 10° to 25°.

In-situ station calibration was discussed and applied in *Granström and Johansson* (2007), but most of the results were based on the statistical method. The Gipsy software was used in the PPP mode to analyze 6 years data from 20 stations in the SWEPOS network and some additional European IGS (International GNSS Service) stations for comparison. It was found that practically all the SWEPOS-stations had a very similar elevation dependent phase residual pattern, which was believed to be due to the similar construction design of the monuments. Irregularities in the azimuth and elevation dependent plots of phase residuals could also be identified as disturbances from nearby objects.

A reasonable conclusion from the studies above could be that the electrical characteristics of a GNSS antenna may change from its calibrated values when installed on a monument. And the effect on positions will probably be relatively small (millimeters) if only one frequency is used, e.g. GPS L1, in high precision applications in limited areas. However, for applications where the ionosphere free linear combination (L3) is used together with the estimation of the tropospheric zenith delay (L3t) the effect may reach centimeter(s). If so, this is an important effect that needs further attention. As an example, the determination of the local tie between various space geodetic techniques at fundamental geodetic stations could be considered. The GPS L1 observable is commonly used together with terrestrial techniques for the determination of the vectors between the reference points of the various instruments (e.g. radio telescope for VLBI) and the GNSS antenna reference point. However, in the IGS, it is not the L1 but the L3t that are used for the analysis. Thus, a bias at the centimeter level may easily be introduced.

Therefore, Lantmäteriet have performed experiments with in-situ station calibration of its permanent reference stations, SWEPOS^{TM} (*Lilje et al*., 2014). The first field campaigns were done in 2009 and 2010, with focus on the original 21 fundamental concrete pillar stations in SWEPOS that serve as the backbone for SWEREF 99 (the national reference frame). One purpose of the calibration is to examine the site-dependent effects on the height determination in SWEREF 99 when the presently available antenna PCO/PCV models are used. Another purpose is to establish corrected PCO/PCV descriptions for antennas mounted at SWEPOS stations as alternatives or complement to those resulting from absolute calibrations of the isolated antenna. The analysis and results from these first campaigns has been reported in *Jarlemark et al*. (2013). A short review of the methodology and key findings are given in chapter 2, 3 and 4.

To keep the time series of the 21 fundamental stations consistent, the antennas of these pillar stations will not be changed as long as they work properly. But these old an-

tennas have a pre-amplifier opening only for the GPS L1 and L2 frequencies and cannot track all new signals such as Galileo and GPS L5 properly. In 2012 a second monument was installed at 19 of the 21 stations with a newer antenna (LEIAR25.R3). To reduce the multipath effects that have been seen from the relatively wide pillar and the large metal plate (*Ning et al*., 2010), a steel grid mast was used for these new monuments (see Fig. 1). Calibration of the new monument relative to the concrete pillars is presented in chapter 5.

In the second part of 2015, six sites were revisited, and in-situ field calibration was performed. The validity of the calibration values from previous experiment could now be tested. Analysis and results are given in chapter 6.

Fig. 1. The SWEPOS site Vänersborg during a station calibration setup in November 2014. An Eccosorb® plate is mounted directly below the visiting choke-ring antennas. Note the typical SWEPOS concrete pillar and the recent steel-grid mast with the LEIAR25.R3 antenna and LEIT radome installed.

2 Surveying campaigns

The first station calibration campaigns started in 2009 and continued in 2010. 12 stations were calibrated during these two years where each station calibration lasted for five days. This first campaign including results has been reported in *Jarlemark et al*. (2013). An overview is given here but for details we refer to the article.

We used three well calibrated antennas on tripods as references in the campaigns. Microwave absorbing material (Eccosorb®) was installed in order to reduce multipath effects from the ground (Fig. 1). The reference antennas (JAVRINGANT and JNSCR_C146-22-1 were used) were placed on markers in a local geodetic network surrounding the concrete pillar where the SWEPOS antenna is installed. The distances between reference antennas and the pillar are of the order of 10 m. The height differences were determined to sub-mm using terrestrial methods. The bench-marks in the local networks are determined using levelling, and the pillar top is determined using total station observations.

Data from the campaigns were analyzed using an in-house software in order to evaluate, and possibly update the existing PCO and PCV models. The benefits of the in-house Matlab software is (among others) that we have full control of the phase residuals and what should be attributed to the antenna on the pillar antenna installation and the

visiting antenna respectively. We also have the possibility to mask off or down weight observations in directions of disturbances.

Data from this first campaign were also analyzed with the Bernese GNSS software with L3t solutions (the L3 ionosphere-free linear combination and estimation of tropospheric delay parameters). The resulting height differences between the reference antennas and the pillar antenna typically deviated by ~10 mm from what was expected according to the terrestrial surveys (*Jarlemark et al*., 2013).

3 PCO and PCV analysis

The height differences in the L3t solutions discussed above suggest that the PCO/PCV models for the antennas on the SWEPOS pillar monuments are not adequate. We therefore aim to quantify the influence of these monuments on the phase observables. In order to accomplish this, we estimated the baseline vectors between the reference and SWEPOS antennas from single differences of the phase observables (e.g. *Hoffman-Wellenhof et al*., 1994). The estimation was performed using an in-house MatLab software.

For each baseline between a SWEPOS monument and a visiting reference antenna, the recorded phase data from the two antennas are subtracted and adjusted for the ambiguous number of cycles recorded (cycle fixing). A small correction for the expected atmospheric delay difference due to height differences between the two antennas in the baseline is also applied. For these short baselines we expect that the remaining atmospheric delay differences, after the correction, typically are smaller than 0.1 mm. The data are also corrected for the antenna PCO and PCV values according to the original description files, determined from absolute calibrations. We assume that the PCO and PCV descriptions of the reference antennas, which were obtained from individual calibrations, give a "correct", bias free, representation of the observed phase (which should be considered as a fairly reasonable approach). Then we can associate deviations in the estimated baselines, as well as systematic signatures in the post-fit residuals, as originating from imperfections in the PCO and PCV of the SWEPOS antenna and its installation. The original baseline vector estimation scheme only contains parameters for one set of coordinates (East, North, Up) per day and one clock difference per epoch. In the results presented here, a 15 s epochs sampling rate was used. The estimation was performed for GPS observations on L1 and L2 separately.

The post-fit residuals did not show significant variation with azimuth angle in the data sets of this paper. They had, on the other hand, significant elevation angle dependence, with different structure on L1 and L2. We sorted the residuals into 2.5° elevation angle bins. The mean values for the data in each bin were taken to represent the PCV error introduced by the SWEPOS antenna. Also, the vertical components of the baseline vectors were slightly different from what was expected from the terrestrial survey; a few mm discrepancies were typically found. These differences were regarded as measures of the errors in the vertical PCO for the SWEPOS antennas. Unfortunately, the horizontal components of the baseline vectors are not as accurately determined by terrestrial meth-

ods in our measurements (due to imperfections in the orientation (rotations) of the local geodetic networks). But from the circular symmetry of the antenna setup, we do not expect any significant horizontal biases.

In addition, a fraction of the phase deviations that originate from PCO or PCV errors can be absorbed into the clock estimate parameters. In order to minimize this effect, we iterated the baseline vector estimation. After the first iteration we made a preliminary updated version of the PCV descriptions for the SWEPOS antennas. We subtracted the PCV errors found from the mean values in the elevation bins from the corresponding components in the original PCO/PCV description of the SWEPOS antennas and made a re-run of the estimation scheme. The resulting new residuals were again sorted into 2.5° bins. The total PCV errors were then taken as the sum of the mean values from the two iterations.

In a later version of the in-house software we have introduced PCV errors as variables directly estimated in the software. They are modeled as a piecewise linear chain of parameters separated by 2.5° in elevation angle. Each parameter is estimated as one value per day. In this software version there is no need for iterations. Tests have shown that the two software versions yield in practice identical results.

4 Results from the in-situ calibration of the pillar antennas

Results from the 2009 and 2010 campaign data are given in detail in *Jarlemark et al*. (2013), where results from 9 sites are presented. The most important findings are repeated below, however with some additional information on uncertainty of the results.

In order to test the methodology and the quality of the observations at the visiting antennas, an initial analysis including just the visiting antennas has been performed. Residuals from Sundsvall and Hässleholm is given in figure 2.

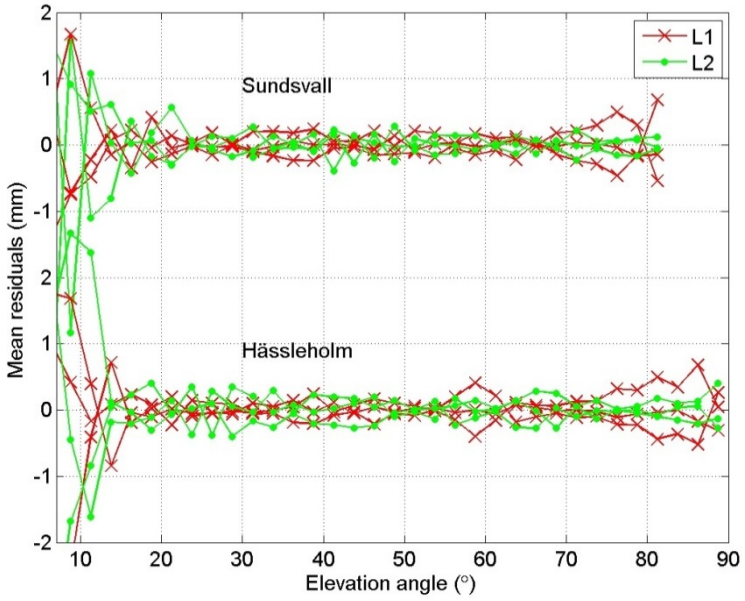

Fig. 2. Phase residuals while computing between only the three reference antennas at two sites. The low noise (>15°) indicate good observations.

The repeatability of the PCV calibration values of the 5 days from the three visiting antennas at SWEPOS station Vänersborg are given in Figure 3 *Left*. The standard deviation is given in Figure 3 *Middle*. The number of observations at different elevations are given in Figure 3 *Right*.

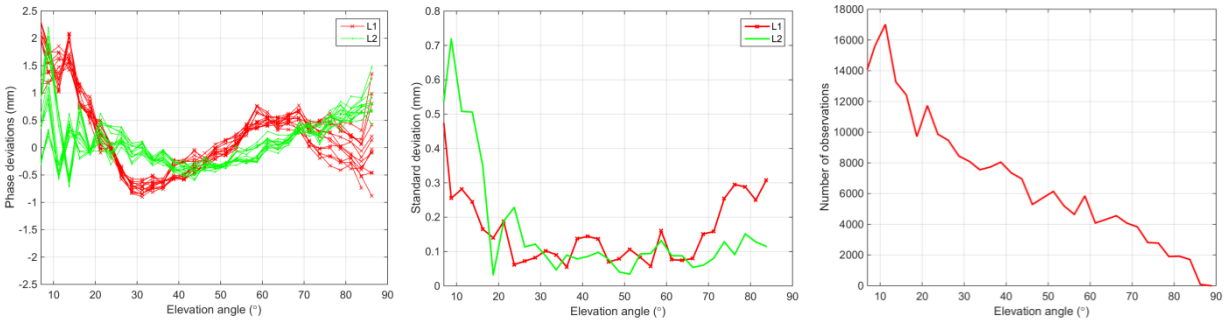

Fig. 3. Results from 5 day in-situ calibration of the SWEPOS station Vänersborg. *Left*: Elevation dependent phase residuals from 5 days and the three reference antennas (15 curves). *Middle*: The standard deviation of the 15 curves of L1 and L2 respectively in *Left* plot (standard uncertainty of the mean is almost 4 times smaller). *Right*: Number of observations plotted to elevation, indicating fewer observations at high elevation.

The elevation dependent mean values of the PCV errors for the nine SWEPOS pillar antennas analyzed are given in Figure 4 Left. The elevation structure of the curves (~1 oscillation over the elevation range 0-90°) is typical for electromagnetic interaction with a surface located ~ ½ wavelength below the antenna (*Elósegui*, 1995). It could therefore be associated with the metal plate (in combination with the top of the concrete pillar) that is located ~0.1 m below the SWEPOS antennas.

The similarities between different stations vertical PCO and PCV errors suggest that a common "monument specific" PCO/PCV description file could be made for the pillar monuments. We therefore formed mean PCV errors for both L1 and L2 in Figure 4, Right. The vertical components of the L1 and L2 PCO were also corrected using the mean values, 0.4 mm and 1.5 mm, found in Table 1. An L3 curve (ionosphere free linear combination of the L1 and L2 observations) is also included (in blue).

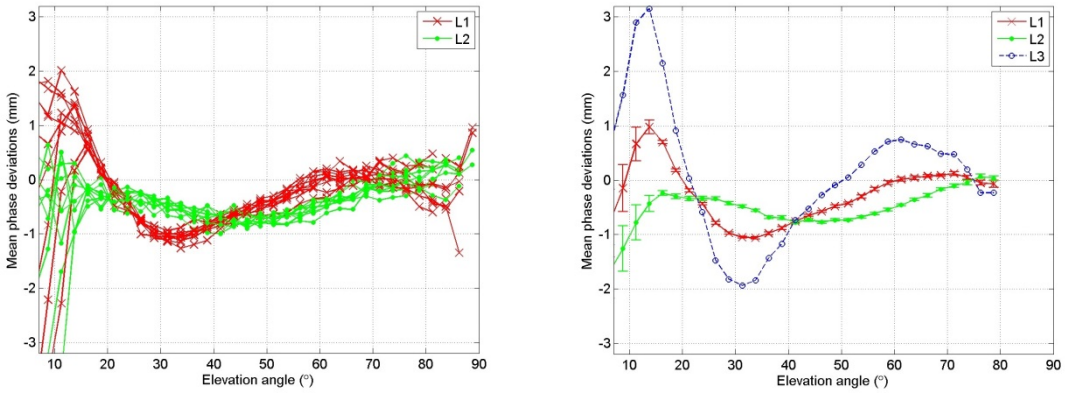

Fig. 4. *Left*: Phase deviations of the nine SWEPOS pillar stations investigated. The deviations are formed by sorting the residuals into 2.5° bins and calculate the mean value for each bin. *Right*: Mean of the phase deviations for the nine SWEPOS stations for L1 and L2 based on the data of the graph to the left. An L3 curve (forming the ionosphere free linear combination of L1 and L2 observations) is also included. Notice the significantly larger amplitude of the L3 curve.

In a L3t estimation where the atmospheric delay is estimated using the L3 data (ionosphere-free) together with coordinates and clock parameters, all these three parameters can potentially absorb an elevation dependent source of error. We again used the in-house software to estimate baseline vectors. This time we added a parameter representing atmospheric delay difference to the scheme. The elevation dependence of the atmospheric delay was modeled with the Niell mapping function, NMF (Niell 1996), and no elevation dependent weighting was applied. For each baseline we made L3 phase differences that were used as observations to the software. An elevation cut off angle of 12° was used, in order to avoid too much disturbances from the surroundings of the reference antennas. The resulting height differences between these L3 estimates and the terrestrial survey as well as the estimated atmospheric delay differences are presented in Table 1 (3rd columns). We repeated the L3t baseline vector estimation scheme but using the updated PCO/PCV description file for the SWEPOS pillar antennas. The results are presented in the last two columns of Table 1. There is still a noticeable variation from station to station (the std value), but the mean values for the height error and atmospheric delay difference is now significantly reduced. (See *Jarlemark et al*. (2013) for details.)

Table 1. Estimated vertical PCO offsets using original and updated PCO/PCV description files for the SWEPOS pillar antennas using L1 and L2 observations (left columns), and the L3t observations (right columns).

	Original antenna model		Updated antenna model		Original antenna model, L3t		Updated antenna model, L3t	
	L1 vertical offset (mm)	L2 vertical offset (mm)	L1 vertical offset (mm)	L2 vertical offset (mm)	Vertical offset (mm)	Atm delay offset (mm)	Vertical offset (mm)	Atm delay offset (mm)
Mean	0.4	1.5	-0.1	0.2	**-12.1**	**3.2**	-0.8	0.1
Std	1.1	1.1	1.1	1.0	2.6	0.5	2.6	0.4

5 Calibration of the new steel grid mast installations

Based on the calibration values we have derived above for the SWEPOS pillar station installations, we “calibrate” the newly installed steel grid mast stations equipped with the LEIAR25.R3 antennas and LEIT radomes, relative to the pillars.

We assume that the derived model is valid for the 19 pillar stations where we have co-located “new” steel grid mast stations. We can then use the pillars to calibrate the antenna installations on the new mast stations. Data from two weeks in 2013 were used to calibrate each mast and antenna pair, and comparison was done to height difference determined using terrestrial surveying techniques (as described in chapter 2). For the LEIAR25.R3 antennas and LEIT radomes on the mast stations, the type calibration values from Geo++ were used in the analysis. The analysis gave distinct deviations from the type-PCV in L1 and L2 according to Figure 5 (left). The average deviations for the PCV deviations in L1 and L2 are given as the red and green curves in Figure 5 (second

left). The deviation is amplified when forming L3 (blue curve). The results from an individual station (Vilhelmina) is given in Figure 5 (right columns).

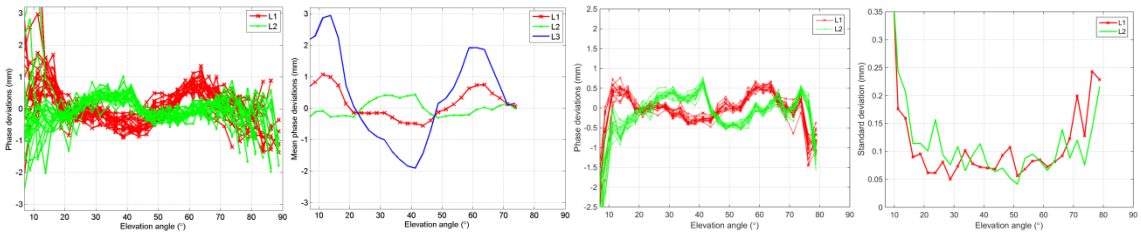

Fig. 5 *Left*: The estimated L1 and L2 phase deviations from the original model PCV for the 19 mast stations studied. *Second left*: The mean of the estimated L1 and L2 phase deviations from the original model PCV, as well as the result when combining them to L3. In the two last plots to the right the repeatability for a single site is given (SWEPOS station Vilhelmina). First the phase residuals for the 14 days of calibration is given. In the rightmost plot the standard deviation is given for the L1 and L2 curves for Vilhelmina (standard uncertainties for the mean values are thus almost 4 times smaller).

The deviation of PCO/PCV for L3 cause a considerable vertical bias (mean value of -11.5 mm) in L3t solutions for the new mast stations, see Table 2.

Table 2. Estimated vertical offsets when using L3t solutions and the original PCO/PCV description file for the steel grid mast antennas.

Station	**Offset (mm)**	**Station**	**Offset (mm)**
Arjeplog	-19.0	Skellefteå	-12.6
Hässleholm	-5.2	Sundsvall	-15.5
Jönköping	-11.0	Sveg	-12.6
Karlstad	-19.2	Umeå	-17.6
Kiruna	-9.0	Vänersborg	-4.4
Leksand	-10.3	Vilhelmina	-8.1
Lovö	-17.4	Visby	-11.5
Mårtsbo	-16.3	Östersund	-3.5
Norrköping	-7.4	Överkalix	-13.9
Oskarshamn	-7.1		
Mean		**-11.5**	
Std		**5.0**	

There is a considerable scatter in the results, standard deviation of 5 mm according to Table 2, despite a ”cleaner” setup when the mast installations are calibrated relative to the pillar stations - the influence from vegetation are limited compared to when temporary calibration antennas on tripods are used. There is some influence due to limitations in the general correction model for the pillar stations, but likely less than the 2.6 mm standard deviation found from the calibration of the pillar stations (Table 1). Using the law of error propagation and subtracting the variance of the estimated offset at the pillars (2.6^2) from the variance of the steel grid masts (5.0^2) gives the standard uncertainty for the mast station installations themselves of 4.2 mm.

6 Re-calibration visits at 6 sites in 2015

In the second part of 2015, six sites were revisited, and site calibration was performed during about 6 days using 3 reference antennas which were individually calibrated at Geo++. The sites have been visited in earlier campaign, giving the possibility to check the performance of the developed PCV/PCO models.

The analysis was done both for the old pillar monuments as well as for the new steel grid mast stations.

6.1 Pillar Stations

The general antenna pillar model derived in chapter 4 was applied.

While analysing the phase residuals we see no major deviations in PCV from the applied model. The noise level is increased at low elevations, probably caused by problems with vegetation around the visiting antennas. There is also an increase in noise at high elevations due to the few observations (due to our location at high latitude – see Fig. 3 *right*).

The antenna heights estimated using L1 and L2 agree to the model at the 1 mm level, and L3 at the 2 mm level, see Table 4. While determining the heights using L3t, a standard deviation of 3.5 mm is achieved. This is somewhat larger than the 2.6 mm in the original calibration. This is probably because of more vegetation in the vicinity of the visiting antenna during this campaign.

Table 4. Estimated vertical offsets from the revisit campaign, when using a general updated model for the pillar antennas.

	L1	**L2**	**L3**	**L3t**
Hässleholm	-2.3	-1.6	-3.3	3.2
Jönköping	-1.3	-1.2	-1.5	2.2
Karlstad	0.7	-0.1	1.7	6.8
Norrköping	-1.5	-0.2	-3.6	4.1
Oskarshamn	-2.0	-1.1	-3.3	-3.6
Vänersborg	-1.0	-0.9	-1.1	1.4
Mean	**-1.2**	**-0.9**	**-1.9**	**2.3**
Std	**1.0**	**0.6**	**2.0**	**3.5**

6.2 Steel grid mast stations

First the developed general antenna mast model from chapter 5 was applied. The mean residuals in figure 6 (left) are reasonable small, with some signature in L1 at 45 to 75 degrees elevation.

The estimated antenna heights from computing using L1 and L2 agrees to the model at the 1 mm level, but increase to 3 mm level for L3, see table 5 (left part). While using L3t, the variations increase to a standard deviation of about 7 mm.

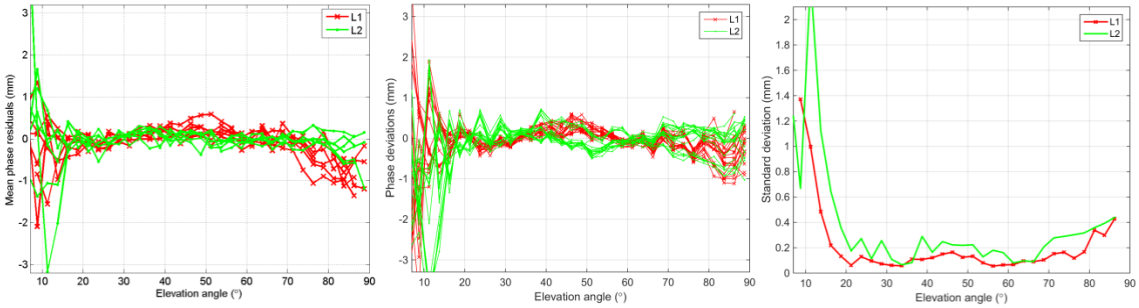

Fig. 6. *Left*: The L1 and L2 mean residuals of the six stations from the revisit campaign, when processing the steel-grid mast data using the model with updated general PCV. *Middle*: Phase residual repeatability of the 7 days with three visiting reference antennas (19 curves for L1 and L2) for SWEPOS site Oskarshamn. *Right*: standard deviation of the curves in *Middle* (standard uncertainties of the mean values are thus about 4 times smaller).

Table 5. Steel grid mast vertical offsets from the revisit campaign. *Left part*; updated general model used. *Right part*; updated model with individual PCO and PCV used.

	General model				**Model with individual PCO and PCV**			
	L1	**L2**	**L3**	**L3t**	**L1**	**L2**	**L3**	**L3t**
Hässleholm	1.6	1.0	2.5	9.8	-0.7	-0.8	-0.7	4.8
Jönköping	-1.1	0.3	-3.3	-4.6	-1.2	-0.2	-2.6	-3.3
Karlstad	-1.5	0.5	-4.6	-4.0	0.9	0.7	1.1	4.2
Norrköping	-0.7	0.5	-2.5	-1.4	-1.3	0.0	-3.2	-5.4
Oskarshamn	0.1	0.6	-0.6	-1.7	-0.9	0.0	-2.4	-5.4
Vänersborg	0.0	-1.9	3.0	10.6	0.3	-0.2	1.2	1.8
Mean	**-0.3**	**0.1**	**-0.9**	**1.5**	**-0.5**	**-0.1**	**-1.1**	**-0.6**
Std	**1.1**	**1.0**	**3.1**	**6.9**	**0.9**	**0.5**	**2.0**	**4.7**

Applying, for each station individually, the suggested PCO and PCV corrections from the work in chapter 5, the scatter in height are reduced for computation using L3 and L3t to about 2 mm and 5 mm respectively (Table 5, right part). These relatively large values may partly be due to problems with vegetation in the vicinity of the calibrating reference antennas.

7 Complications when using the applied calibration method

In order to be valid when used in the field, the models of the antenna PCO and PCV pattern derived from absolute calibrations must be preserved when mounted in the field on a tripod.

We have therefore used microwave absorbing material at the calibrating antennas in order to limit influence of multipath. It has, however, been reported that also the use of such material may cause some changes of the antenna phase center variation (*Aerts et al.*, 2016). The L3t results presented above have the highest influence of the expected pattern errors. Preliminary analysis indicate that L3t heights could have been influenced on the level of a couple mm.

While performing in-situ calibration in the field, we would like to receive undisturbed observations at the calibration antennas down to 10° elevation (and beyond) in order to be able to calibrate the PCV of the visited station. However, the visiting antennas usually do get a relatively low setup, and at several stations we do have a "growing" problem with vegetation in the low elevation signal path.

8 Summary and discussion

When using the presently available antenna models (type mean), GNSS determination of the height difference between the SWEPOS pillar antennas and the surrounding reference antennas gave ~ 10 mm too low heights for the SWEPOS antennas. This error was derived from a comparison with conventional terrestrial surveys. The result varied significantly between days, and also between different processing strategies. PCO/PCV errors derived from GNSS phase differences showed elevation angle signatures that may cause the lower and larger values for the estimated height component and atmospheric delay, respectively. Electromagnetic coupling between the antenna and a metal plate below the antennas is probably contributing to the systematic PCO/PCV errors found.

Simulations using the derived PCO/PCV errors suggest 7–16 mm lower heights due to these errors, i.e. approximately of the same sizes as was found in the "real" GNSS height determination. In the simulations the PCO/PCV descriptions of the reference antennas were considered to be known after being calibrated. During calibration they were mounted on a "robot arm" that might have introduced systematic errors. The possible size of this effect is, at present, unknown to us. It has been suggested that in-situ calibration could be done with antennas mounted on something that mimic the top of the robot arm during local calibrations in order to reduce the possible effect (*Wübbena et al*., 2010).

Our results presented here have implications on a number of practical applications. To be mentioned is determination of the "local tie" between the GNSS reference point and the one from other instrumentation at fundamental geodetic stations. Usually, the L1 observable is used while observing the local GNSS networks in order to get as precise results as possible. But when used in the IGS, the L3 (ionosphere-free) observable is used and also solving for troposphere delays. Thus, an error at the 1 cm level is easily introduced due to PCO/PCV errors.

Although many details of the practical field calibration remain to be improved, we have shown that in-situ station calibration is feasible and gives a better understanding of antenna related issues in precise GNSS applications.

Acknowledgements

We thank Ulla Kallio and an anonymous reviewer for suggestions that have improved the manuscript considerably.

References

Aerts, W., C. Bruyninx and P. Defraigne, 2016. On the influence of RF absorbing material on the GNSS position. *GPS Solution*, **20**(1), 1–7. DOI 10.1007/s10291-014-0428-y.

Elósegui, P., J.L. Davis, R.T.K. Jaldehag, J.M. Johansson, A.E. Niell and I.I. Shapiro, 1995. Geodesy using the Global Positioning System: The effects of signal scattering on estimates of site position. *J. Geophys. Res*., Vol. **100**, No. B6, pp 9921-9934.

Granström, C. and J.M. Johansson, 2007. Site-Dependent Effects in in High Accuracy Applications of GNSS. Presented at the Symposium of the IAG sub commission for Europe (EUREF), 6–8 June 2007, London. http://www.euref.eu/symposia/2007London/05-02-lidberg.pdf (Sited 2019-03-18).

Hoffman-Wellenhof, B., H. Lichtenegger and J. Collins, 1994. *GPS: Theory and practice*, Springer Verlag, New York.

Jarlemark, P., M. Lidberg, C. Kempe, L. Jivall, J.M. Johansson and T. Ning, 2013. Station calibration of the SWEPOS™ network (revised version 2013-09-25). Proceedings of the EUREF symposium in Saint-Mandé, June 6–8, 2012, http://www.euref.eu/symposia/2012Paris/P-02-p-Kempe.pdf (Sited 2017-10-14).

Lidberg, M., P. Jarlemark, K. Ohlsson and J.M. Johansson, 2016. Station calibration of the SWEPOS GNSS network. Presented at the Symposium of the IAG sub commission for Europe (EUREF), 25–27 May 2016, San Sebastian, Spain. http://www.euref.eu/symposia/2016SanSebastian/03-04-Lidberg.pdf (Sited 2019-03-19).

Lilje, M., P. Wiklund and G. Hedling, 2014. The Use of GNSS in Sweden and the National CORS Network SWEPOS. FIG Congress 2014 Engaging the Challenges – Enhancing the Relevance Kuala Lumpur, Malaysia 16–21 June 2014. http://www.fig.net/resources/proceedings/fig_proceedings/fig2014/papers/ts08a/TS08A_lilje_wiklund_et_al_7019.pdf (Sited 2019-03-17).

Niell, A.E. 1996. Global mapping functions for the atmosphere delay at radio wavelengths. *J. Geophys. Res*. **101**, 3227–3246.

Ning, T., G. Elgered and J.M. Johansson, 2010. The impact of microwave absorber and radome geometries on GNSS measurements of station coordinates and atmospheric water vapour. *Adv. Space Res*., Vol. **47**, no. 2, 186–196, doi:10.1016/j.asr.2010.06.023.

Rothacher, M. and G. Mader, 2003. Receiver and satellite antenna phase center offsets and variations. In: Tétreault, P., Neilan, R., Gowey, K. (eds.) Proceedings of the Network, Data and Analysis Centre 2002 Workshop, pp. 141–152, Ottawa. http://www.igs.org/assets/legacy-content/02_ott/session_8.pdf.

Schmid, R., G. Mader and T. Herring, 2005. From relative to absolute antenna phase center corrections. In: Meindl, M. (ed.) Proceedings of the IGS Workshop and Symposium 2004, Bern, pp. 209–219. ftp://igs.ensg.ign.fr/pub/igs/igscb/resource/pubs/04_rtberne/cdrom/Session10/10_0_Mader.pdf.

Wübbena, G., M. Schmitz and N. Matzke, 2010. On GNSS in-situ Station Calibration of Near-Field Multipath. International Symposium on GNSS, Space-based and Ground-based Augmentation Systems and Applications, November 29–30, 2010, Brussels.

Wübbena, G. and M. Schmitz, 2011, *On GNSS Station Calibration of Antenna Near-Field Effects in RTK-Networks*. International Symposium on GNSS, Space-based and Ground-based Augmentation Systems and Applications, October 10–11, 2011, Berlin.